Published in final edited form as:
Pediatr Blood Cancer. 2012 February ; 58(2): 173–180. doi:10.1002/pbc.23015.

Preclincial Testing of Sorafenib and RAD001 in the *Nf* $^{fl/fl}$*;DhhCre* mouse model of plexiform neurofibroma using magnetic resonance imaging

Jianqiang Wu, M.D.[1], **Eva Dombi, M.D**[2], **Edwin Jousma, M.S.**[1], **R. Scott Dunn, B.S.**[3], **Diana Lindquist, Ph.D.**[3], **Beverly M. Schnell, Ph.D.**[4], **Mi-Ok Kim, Ph.D.**[4], **AeRang Kim, M.D.**[2], **Brigitte C. Widemann, M.D.**[2], **Timothy P. Cripe, M.D., Ph.D.**[1], and **Nancy Ratner, Ph.D.**[1]

[1]Divisions of Experimental Hematology and Cancer Biology, Department of Pediatrics, Cincinnati Children's Hospital Research Foundation, Cincinnati Children's Hospital Medical Center, 3333 Burnet Ave., Cincinnati, OH 45229, USA

[2]Pediatric Oncology Branch, National Cancer Institute, CRC 1-3872, 10 Center Drive, Bethesda, MD 20892, USA

[3]Department of Radiology, Cincinnati Children's Hospital Research Foundation, Cincinnati Children's Hospital Medical Center, 3333 Burnet Ave., Cincinnati, OH 45229, USA

[4]Divisions of Biostatistics and Epidemiology, Department of Pediatrics, Cincinnati Children's Hospital Research Foundation, Cincinnati Children's Hospital Medical Center, 3333 Burnet Ave., Cincinnati, OH 45229, USA

Abstract

Background—Neurofibromatosis type 1 (NF1) is an inherited disease predisposing affected patients to variable numbers of benign neurofibromas. To date there are no effective chemotherapeutic drugs available for this slow growing tumor. Molecularly targeted agents that aim to slow neurofibroma growth are being tested in clinical trials. So preclinical models for testing potential therapies are urgently needed to prioritize drugs for clinical trials of neurofibromas.

Procedure—We used magnetic resonance imaging (MRI) to monitor neurofibroma development in the *Nf1*$^{flox/flox}$*;DhhCre* mouse model of GEM grade I neurofibroma. Based on studies implicating mTOR and Raf signaling in NF1 mutant cells, we tested the therapeutic effect of RAD001 and Sorafenib in this model. Mice were scanned to establish growth rate followed by eight weeks of drug treatment, then re-imaged after the last dose of drug treatment. Tumor volumes were determined by volumetric measurement.

Results—We found that rate of tumor growth varied among mice, as it does in human patients. RAD001 inhibited its predicted target pS6K, yet there was no significant decrease in the tumor volume in RAD001 treated mice compared to the vehicle control group. Sorafenib inhibited cyclinD1 expression and cell proliferation in tumors, and volumetric measurements identified significant decreases in tumor volume in some mice.

Conclusion—The data demonstrate that volumetric MRI analysis can be used to monitor the therapeutic effect in the pre-clinical neurofibroma drug screening, and suggest that Sorafenib might have clinical activity in some neurofibromas.

Author for correspondence: Nancy Ratner: Tel: (513)-636-9469, Fax: (513)-636-1446, nancy.ratner@cchmc.org.

Keywords

Neurofibromatosis type 1; Neurofibroma; Magnetic resonance imaging; Sorafenib; RAD001

Introduction

Plexiform neurofibromas develop in 25 - 30% of children with neurofibromatosis type 1 (NF1) [1]. Plexiform neurofibromas are benign peripheral nerve Schwann cell tumors that can cause disfigurement, nerve compression, and distortion or infiltration of adjacent structures, and can compress vital structures causing mortality [2]. The only current standard neurofibroma therapy is surgery, which is not always feasible as it necessitates removal of tumors of neurofibroma- integrated nerves. Even after surgery many patients experience tumor recurrence [2]. To date there are no effective chemotherapeutic drugs available for this slow growing tumor, so molecularly targeted agents that aim to slow plexiform neurofibroma growth are being tested in clinical trials. The activity of agents is being analyzed using sequential volumetric imaging of tumors using magnetic resonance imaging (MRI), the most sensitive method available [3]. This method allows to reproducibly (coefficient of variation ≤ 5%) detect smaller changes in plexiform neurofibroma size compared to standard solid tumor response criteria. In currently ongoing clinical trials disease progression is defined as a ≥20% increase, and response as a ≥20% decrease in plexiform neurofibroma volume from baseline prior to initiation of investigational treatments [3-4]. In a mouse model of neurofibroma formation, neurofibroma growth was monitored by Positron Emission Tomography (PET) scanning [5]. Although PET may be more sensitive than MRI for detecting smaller lesions, it cannot directly measure tumor size and is more expensive than MRI. It would be useful to prioritize drugs for clinical testing in a mouse model in preclinical drug trials by monitoring tumor growth over time using sequential volumetric imaging.

NF1 is a tumor suppressor gene that encodes a GTPase activating protein (GAP) for Ras proteins [6]. Complete loss of *NF1* in neurofibroma Schwann cells leads to increased levels of Ras-GTP [7] known to activate Raf kinase, phosphatidylinositol 3′-kinase (PI3K), and other signals, regulating cell proliferation, survival and cell death [8]. Research focused on the biology of NF1 and pathogenesis of plexiform neurofibroma and their malignant peripheral nerve sheath tumors (MPNSTs) has identified potential targets including Ras itself, Raf kinase, angiogenesis, growth factor receptors, and mammalian target of rapamycin (mTOR) [9-10]. For example, S6K1 is activated in MPSNT cells with NF1 mutations, and this response is attenuated by rapamycin in MPNST cell lines, MPNST xenografts, and in a genetic engineered mouse model [11-12]. In a mouse sarcoma model in which *Nf1* and *p53* mutations are in cis on mouse chromosome 11, mice treated with rapamycin showed delayed tumor formation [11]. On this basis, a Phase II trial of rapamycin in plexiform neurofibromas is ongoing.

We developed the $Nf1^{flox/flox}$;*DhhCre* neurofibroma mouse model in which loss of both *Nf1* alleles in developing Schwann cell precursors at embryonic day 12.5 causes neurofibroma formation in adult mice [13]. The tumors show the loss of axon Schwann cell interaction, mast cell accumulation, and fibrosis, which are characteristics of human plexiform neurofibromas. Four – 20 tumors arise in each mouse and at sacrifice each tumor is >10 mm^3. We reasoned that MRI with volumetric analysis could be used to monitor neurofibroma development in the $Nf1^{flox/flox}$;*DhhCre* mouse model. Based on previous studies implicating mTOR signaling and Raf signaling in *NF1* mutant cells, we tested the therapeutic effect of the rapamycin analog RAD001 [14], an mTOR inhibitor, and Sorafenib, a multi-targeted kinase inhibitor that was originally developed as a raf kinase inhibitor [15],

in this model. We demonstrate that volumetric MRI can be used to monitor neurofibroma growth in mice. We also show that RAD001 does not decrease neurofibroma growth, while Sorafenib has significant therapeutic effect on some neurofibromas in this model.

Methods

Mouse

We housed mice in temperature- and humidity-controlled facilities on a 12-hour dark-light cycle with free access to food and water as described previously [13]. The animal care and use committee of Cincinnati Children's Hospital Medical Center approved all animal use. The mice were in a mixed C57/129/FVBN strain background and were interbred to obtain the expected genotype. Mouse genotyping has been described [13].

Chemicals

RAD001 and vehicle carrier were obtained from Novartis Pharmaceuticals Corporation (East Hanover, NJ). RAD001 was in a microemulsion solvent that was diluted to 3 parts 2% carboxyl methylcellulose and 2 parts 6% captisol for in vivo usage [16].

Sorafenib was purchased from LC Laboratories (Woburn, MA). Sorafenib was dissolved in 50% cremophor EL (Sigma, St. Louis, MO) – 50% ethanol (Pharmaco Products, Brookfield, Conn). The mixture was sonicated for 1-2 minutes on ice to dissolve Sorafenib. Once in solution, the aqueous component (75% water) was gradually added and diluted to generate the final dosing solution. Each dose was weighed and stored in dry form away from light and was dissolved to liquid form immediately prior to oral gavage.

Preclinical paradigms

RAD001: We used RAD001 instead of its analog rapamycin because of improved oral availability [17]. The RAD001 dose was chosen based on studies in which daily oral administration of RAD001 at 10 mg/kg produced transient tumor stasis in an MPNST xenograft model [12] and after a preliminary tolerated dose study in the neurofibroma mouse model (not shown). Seven-month old *Nf1*$^{flox/flox}$*;DhhCre* mice (n=15) were imaged by MRI followed by daily oral gavage for 8 weeks of RAD001 (10 mg/kg) diluted in 3 vehicle carrier. Vehicle-treated mice (n=5) were gavaged daily with the same solution lacking RAD001. These animals were re-imaged by MRI at 9 months of age after the completion of the last dose.

For the Sorafenib trial, 9-month old *Nf1*$^{flox/flox}$*;DhhCre* mice (n=10) were imaged by MRI then treated with Sorafenib (45mg/kg) daily by oral gavage. This Sorafenib dose was chosen based on preclinical studies in which daily oral administration of Sorafenib at 30 to 60 mg/kg produced complete tumor stasis during treatment in five of six tumor models tested [15,18] and a preliminary maximum tolerated dose test in this neurofibroma mouse model (not shown). A control group (n=4) received 200 μl of vehicle daily.

Magnetic resonance imaging (MRI)

Mice were anesthetized with 5% isoflurane in air and maintained during imaging on 1% isoflurane in air. Mice were positioned in a linear volume transmit/receive coil using a bite bar to secure their heads. Respiration rate and temperature were monitored with a Model 1025 monitoring and gating system from Small Animal Instruments, Inc. The respiration rate was around 100 breaths/min and the temperature was set to 32°C. All data were acquired with a 7T Bruker Biospec system equipped with 400 G/cm gradients. Localizer images were acquired in 3 planes to position the 3D volume. Fat-suppressed 3D Rapid Acquisition with Refocused Echo (RARE) data were acquired with an effective echo time of

35.39 ms, repetition time of 1000 ms, 1 average, a field-of-view of 51.2 mm × 25.6 mm × 26.5 mm and a matrix size of 256 × 128 × 128. Respiratory gating was used to minimize motion artifacts. The total scan time for each mouse at each time point was approximately 30 minutes.

Tumor volumetric measurement

To determine the reproducibility of the volumetric MRI analysis in tumor bearing mice, one observer (ED) applied the method to the tumors of 10 randomly selected mice on three different days. We obtained mouse MRIs at age of 4, 6, 8 10 and 12 months for a natural history study; at age of 6, 7 and 9 months for the RAD001 treatment groups; and at age 5, 7, 9 and 11 months for the Sorafenib treatment groups. On the above described 3D RARE sequence, the plexiform neurofibromas appear bright in contrast to most other tissues. Medx software (Medical Numerics, Inc., Germantown, MD) was used for volumetric analysis. One observer (ED) manually outlined lesions on each MRI slice containing tumor. Tumor on the left and right side of each mouse was measured separately at the cervical and thoracic levels, where the bulk of tumor was identified. Smaller cauda equine tumors were not included in the analysis, as the resolution in this region limited accuracy. Measurement error increases for tumors with volumes $<10mm^3$, therefore, we report only tumors with volumes $>10mm^3$. The tumor criteria were based on image resolution and MRI section slice thickness similar to those described previously [3]. The program calculated tumor volume from the area of graphic outline and MRI slice thickness. All volumes are reported as combined tumor volume in an individual mouse.

Western blotting

Tumor proteins were extracted using extraction buffer (20 mM$NaPO_4$, 150 mM NaCl, 2 mM$MgCl_2$, 0.1% Nonidet P-40, 10% glycerol, 10 mM sodium fluoride, 0.1 mM sodium orthovanadate, 10 mM sodium pyrophosphate, 100 μM phenylasine oxide, 10 nM okadaic acid, 1 mM dithiothreitol, 10 μg/ml leupeptin, 10 μg/ml aprotinin, 10 μg/ml pepstatin, 10 μg/ml tosyl-L-phenylalanine chloromethyl ketone, and 10 μg/ml N^{α}-tosyl-L-lysine chloromethyl ketone). Protein concentration was estimated using Coomassie® Plus Protein Assay Reagent [19]. Proteins (50 μg/lane) were separated by sodium dodecyl sulfate (SDS)-polyacrylamide gel electrophoresis on 4–20% tris-glycine gel (Invitrogen, Carlsbad, CA) and electrotransferred to polyvinylidene diflouride membrane. Membranes were blocked with 5% nonfat milk + 0.1% TBST to minimize nonspecific binding. Antibodies recognizing pERK, ERK, CyclinD1, pS6K(ser240/244), total S6, p4E-BP1, total 4E-BP1, and β-actin (Cell Signaling, Danvers, MA) were detected by incubation of the membrane with specific antibodies. Antibody binding to the membrane was visualized using a chemiluminescent detection system (ECL, Amersham, Arlington Heights, IL). The bands obtained were quantified by Kodak 1D Imagine Analysis Software (Eastman Kodak Company, IL). Anti-β-Actin was used as a loading control. At least three different tumor lysates were analyzed for each antigen.

Immunohistochemistry

Immunohistochemistry on tumor sections was performed as described previously [20]. Briefly, following deparaffinization and rehydration, we permeabilized sections with 0.2% TX 100 and blocked with 10% normal serum for one hour at room temperature. Primary antibodies were: Ki67, Caspase 3 (Cell Signaling, Danvers, MA), secondary incubations were with host-appropriate secondary antibodies. We acquired microscopic images with Openlab software suites on a Zeiss Axiovert 200.

Pharmacokinetic analysis

Samples were prepared and quantified using a validated HPLC/MS/MS method adapted from an assay developed by Jain et al [21]. The lower limit of quantification was 5 ng/mL. Plasma samples were drawn at times 0.5, 1, 2, 4, 8 hours post Sorafenib dose on day 6. Only one time point was sampled in each mouse and each time point was sampled in three mice.

Statistical analysis

Data shown in the text is presented in tumor volume in mm3. In the plots, data is presented centered at the last pre-treatment value within each mouse. To derive p values, we conducted a random effects model analysis on the log transformed tumor volume data [22] using SAS mixed procedure. The log transformation stabilized the variability of data across time. Tumors grew linearly on a logarithmic scale over the study period in the control group within each mouse and the individual linear growth trajectories were estimated by random coefficients linear regression. We allowed the slope of the linear growth in the treatment groups to be adjusted in the post treatment period. A significantly negative yet small adjustment in the slope indicates reduced growth rate, while a significantly negative and large adjustment indicates tumor shrinkage. The linear random coefficients models accounted for different measurement time points across treatment groups and variability in the growth trajectory across mice. Results are summarized by the plots of mean tumor growth trajectories. To compare statistical significance to data obtained in clinical trials, we also used Pearson's χ^2 test of medians.

Results

Natural History of neurofibroma in the *Nf1$^{flox/flox}$;DhhCre* mouse model

We used magnetic resonance imaging (MRI) to study tumors in the *Nf1$^{flox/flox}$;DhhCre* mouse model. The MRI image characteristics of the *Nf1$^{flox/flox}$;DhhCre* neurofibromas strongly resembled those of human neurofibromas as shown in Figure 1. As shown in the lower panels, the tumors could be distinguished from other tissues and could be outlined for use in volumetric measurement.

The median volume of tumors used to determine the reproducibility of the volumetric MRI analysis was 65.6 mm^3 (range, 12.5-231.8 mm^3), and the coefficient of variation (CV=standard deviation/mean) for repeated analysis of the same tumor by different observers was 5.7% (range 0.7-10.8%). The CV was less than 10% for all but the two smallest tumors (12.5 mm^3 and 27.7 mm^3) analyzed.

Tumor growth was determined by volumetric measurement [4]. Mice (n=5) were repeatedly imaged at 2 month intervals from 4 - 12 months of age months using a Bruker 7.0T MRI (Figure 2A). All five mice had developed tumors by four months of age, and tumors continued to increase in size. Due to imaging artifact, one animal was excluded from volumetric analysis. Figure 2B shows coronal and axial images of one mouse at 6, 8, and 12 months of age, demonstrating the visible increase in tumor size. A group of 20 mice including those used in the natural history study (n = 5), RAD001 study (n= 4), Sorafenib study (n=4), and other studies (n=7) were pooled and evaluated for growth over time as controls (Figure 2C). Similar to what has been observed for human neurofibromas [4], the growth rate of GEM grade I neurofibromas varied between mice, but appeared constant within individual mice.

About 10% of *Nf1$^{flox/flox}$;DhhCre* mice developed large tumor nodules underneath the dermis (Supplemental Figure 1). On histopathology, these tumor nodules showed

characteristic GEM-neurofibroma grade 1 (not shown). These tumors sometimes eroded the overlying skin due to inflammatory reaction and were not included in our analyses.

RAD001 has no effect on inhibiting neurofibroma growth in *Nf1$^{flox/flox}$;DhhCre* mice

To investigate the utility of the *Nf1$^{flox/flox}$;DhhCre* neurofibroma mouse model as a preclinical model we first chose to determine the effect of RAD001 as a single agent. Mice (n=15) born in a cohort within one month of each other were pooled and scanned in a group (beginning at 5 – 6 months of age). One month later they were scanned again and then randomized to control (n = 5) and treatment (n = 10) trial arms. Treatment consisted of eight weeks of daily oral gavage at a dose of 10mg/kg. Mouse weights were obtained twice weekly. Mice were re-imaged after the last dose of drug (Figure 3A). All mice survived the 8 weeks of treatment without lethargy, dehydration or significant weight loss (<5%). Pharmacodynamic measure of efficacy used western blotting for the mTOR effector S6 kinase in tumor lysates taken 2 hours after the final dose of RAD001. RAD001 treatment had the predicted effect on mTOR pathway activation *in vivo*, shown by decreased activation (phosphorylation) of S6 kinase. However, phosphorylation of another mTOR effector, 4E-BP1, was decreased in RAD001 treated tumors as compared to controls, indicating its activation (Figure 3B) [23]. Consistent with this result in one of two tumors, a band shift to lower mobility was observed on RAD001 exposure. Thus, RAD001 treatment of neurofibromas completely inhibits the activation of p70 S6 kinase but seems to slightly decrease phosphorylation (activate) 4E-BP1 in response to RAD001.

Tumor volumes were determined by volumetric measurement at each time point. As noted above, tumor growth rates varied among mice. There was no significant decrease in tumor volume growth rate in RAD001 treated mice (n=10) compared to the vehicle control group (n=5, and pooled controls p=0.36; Supplemental Figure 2) random effects model analysis or Pearson's χ^2 test of medians (Figure 3C. D; Supplemental Table 1 and 2). We also did not detect a difference in cell apoptosis in RAD001 treated mice compared to control treatment in neurofibroma paraffin sections by TUNEL assay. We did not detect any change in cyclin D1 or active caspase 3 by Western blot compared to control tumors (not shown).

Sorafenib significantly decreases the neurofibroma growth rate in *Nf1$^{flox/flox}$;DhhCre* mice

To test the therapeutic effect of Sorafenib, a multi-targeted kinase inhibitor that was originally developed as a raf kinase inhibitor, on neurofibroma growth, we treated mice (n=9) with Sorafenib daily or vehicle control (n=4) by daily oral gavage. To ensure that growth rate was accurately represented, an additional scan was included prior to onset of treatment. Thus mice were scanned at 5, 7, and 9 months to establish tumor growth rate. This additional scan demonstrated a constant growth rate, indicating that the intermediate scan is not necessary. The 9 month scan was followed by eight weeks of drug treatment by daily oral gavage. Mice were re-imaged after the last dose of Sorafenib at 11 months of age. Tumor volumes were determined by volumetric measurement. All mice survived the 8 weeks of treatment without weight loss or other obvious side effects.

We monitored plasma drug concentration at various times after oral Sorafenib administration. Sorafenib was readily absorbed and measurable. The median Sorafenib concentration was 23.7 μg/mL (range 16.6 to 945 μg/mL) (Figure 4D). Peak exposure was at 1 hour and drug was maintained through 8 hours (Figure 4D) as previously described [24].

We observed significant decreases in tumor volume (negative slope) in 5 of 9 Sorafenib treated mice (Figure 4C). One mouse receiving Sorafenib stabilized, while 3 others continued to grow with unchanged growth rate. All vehicle control mice had tumors that continued to grow throughout the experiment excluding a carrier effect. The difference

between Sorafenib and vehicle controls was significant ($p<0.05$; Supplemental Figure 2). Pharmacodynamic measurement of Sorafenib efficacy was monitored indirectly by levels of cyclin D1. Western blots showed that Sorafenib inhibited cyclinD1 expression in two of the three evaluated tumor lysates taken 1 hour after the final dose of Sorafenib (Figure 4B). We also found that pERK expression levels were elevated in these two tumors. Intriguingly, cyclin D1 decreased and PERK increased only in the two tumors from mice which responded to Sorafenib treatment with decreased tumor volume (Figure 4B).

To assess the mechanism underlying Sorafenib treatment, we determined if Sorafenib treatment resulted in increased apoptosis and/or decreased proliferation within the neurofibroma specimens by staining active caspase 3 (apoptosis) and ki67 (proliferation). We observed a decrease in the number of ki67-positive cells in Sorafenib treated neurofibromas that were taken out from the mice 1 hour after the final dose of Sorafenib ($p<0.05$, Figure 5). We did not detect differences in active caspase 3 between Sorafenib and vehicle treated mouse neurofibromas by western blot (not shown). We also did not identify differences in endothelial cell number per high powered field between groups monitored using anti-mouse endothelial cell antibody (not shown).

Discussion

Plexiform neurofibroma is one of the most debilitating complications of NF1 and is associated with substantial significant morbidity [2]. A preclinical model predicting activity would be useful to prioritize clinical trials for investigational targeted agents in patients with NF1 and plexiform neurofibroma. In the *Nf1$^{flox/flox}$;DhhCre* mouse model GEM grade I neurofibromas form in 100% of mice and recapitulate the histology and imaging characteristics of human neurofibromas [13]. In patients, neurofibromas develop along nerve roots and adjacent peripheral nerves, paraspinally, and in deep or superficial locations. Our use of 7 Tesla small-animal MRI enabled our conclusion that the *Nf1$^{flox/flox}$;DhhCre* mouse model mimics mainly the paraspinal phenotype, with tumors predominantly related to the cervical and thoracic spine. We assessed tumor growth rate in the *Nf1$^{flox/flox}$;DhhCre* mouse model using volumetric MRI analysis. The same volumetric measurement technique is in use in ongoing clinical trials and has been proven to sensitively detect small changes in tumor size over time [3-4]. The reproducibility of this method is similar for tumors in mice and humans, and thus the response criteria used in human trials can be applied to the preclinical evaluation in mice. In humans, growth rate varies between patients but appears to be consistent within an individual. Similarly, in the mouse model we identified fast and slow growing tumors, and steady growth for individual tumors. However, in patients with NF1 enrolling in clinical trials most rapid plexiform neurofibroma growth was in young children; older patients typically had little or no growth [4]. In contrast, in the *Nf1$^{flox/flox}$;DhhCre* mouse model, tumors are visible by 4 months on MRI and continue to grow until mice require sacrifice due to spinal cord compression at around 1 year.

We scanned untreated and carrier treated mice at numerous intervals. Based on tumor natural history, we suggest that future preclinical trials using this model will best be accomplished by imaging mice at 5 and 7 months, then using a 2 months treatment followed by a final scan. This paradigm takes into account both the continuous growth of tumors in the model and the time of significant death of *Nf1$^{flox/flox}$;DhhCre* mice, occurring mainly after 9 months of age. Because in individual mice tumor size and growth rate differ, another possible paradigm would be to measure tumor growth rate and only treat mice with large tumors, or tumors of roughly the same size. The fact that we have no evidence that large and small tumors respond differently to drugs argues against this approach, and such a restriction would not reflect the heterogeneity of patients seen in clinical settings.

The predictable neurofibroma growth rate in the *Nf1$^{flox/flox}$;DhhCre* mouse model enabled pre-clinical drug screening. We did not detect discernable effects on tumor growth, tumor cell proliferation, or cell apoptosis on RAD001 treated mice. Similarly, sirolimus (rapamycin) was not effective in shrinking non-progressive plexiform neurofibromas in a Phase 2 trial in children and adults with NF1 and inoperable plexiform neurofibromas. Whether sirolimus prolongs time to progression in subjects with progressive plexiform neurofibromas remains to be determined, and we await trial results with interest [25]. Mouse tumor cells had adequate exposure to RAD001, as neurofibroma pS6 kinase was blocked by exposure to RAD001. It is known that in some systems mTOR blockade can cause feedback activation of Akt activity [26], and it remains possible that this or alternative compensatory mechanisms might account for the failure of RAD001 to block neurofibroma growth. Mechanisms of drug resistance (cell autonomous and/or non-cell autonomous) in many tumors will be an interesting avenue for follow-up studies.

Sorafenib is a multi-targeted kinase inhibitor being tested in a Phase I trial in pediatric patients with NF1 and plexiform neurofibroma. Mice exposed to Sorafenib with tumor growth inhibition also showed decreased expression of the cell cycle regulator cyclin D1, consistent with an effect on tumor growth. Sorafenib inhibited tumor cell proliferation, as attested by immunostaining. The target(s) of Sorafenib in this model are not clear. Raf is predicted to be activated downstream of Ras activation caused by *NF1* loss. Tumor lysates showed increased pERK expression, likely due to a negative feedback loop caused by Raf kinase inhibition [26-29]. Sorafenib also inhibits activity of receptors implicated in neurofibroma cells including c-kit, VGFR2, VGFR3, platelet-derived growth factor receptor ß, and Flt-3, one or more of which might account for some effects of Sorafenib on individual tumors [15]. The reason that 5 of 9 mice responded to Sorafenib exposure by tumor shrinkage while 4 of 9 did not is unknown. Because the mouse strain is a mixed genetic background, there may be co-modifier genes that differ among the animals that alter drug metabolism or target sensitivity, possibilities supported by the variability seen in our individual pharmacodynamic and pharmacokinetic data (Figure 4B and 4D, respectively). Drug penetration into different tumor sites may also vary among mice because of the blood-tumor barrier, or interstitial pressure on selected tumors. Tissue drug levels and pharmacodynamic studies of tumor tissue will be of interest in future preclinical neurofibroma trial design.

Our data demonstrate that Sorafenib can reduce the growth of certain neurofibromas and suggest that Sorafenib might have clinical therapeutic effects on neurofibromas. More importantly, our data show that the *Nf1$^{flox/flox}$;DhhCre* mice are useful to monitor tumor response to targeted therapeutics, indicating the potential usage of this model for preclinical drug screening.

Supplementary Material

Refer to Web version on PubMed Central for supplementary material.

Acknowledgments

This work was supported by the Children's Tumor Foundation NF Preclinical Consortium (TPC and NR), NIH NS28840 (NR), and P50 NS057531 9 (NR). The authors thank the NF Preclinical Consortium members and its Advisory Board for extensive discussions aiding in planning of the experiments. We thank Mr. David W. Eaves and Ms. Deanna Patmore for their endeavors on the mouse work.

References

1. Ferner RE. Neurofibromatosis 1. Eur J Hum Genet. 2007; 15(2):131–138. [PubMed: 16957683]

2. Boyd KP, Korf BR, Theos A. Neurofibromatosis type 1. J Am Acad Dermatol. 2009; 61(1):1–14. [PubMed: 19539839]
3. Solomon J, Warren K, Dombi E, et al. Automated detection and volume measurement of plexiform neurofibromas in neurofibromatosis 1 using magnetic resonance imaging. Comput Med Imaging Graph. 2004; 28(5):257–265. [PubMed: 15249071]
4. Dombi E, Solomon J, Gillespie AJ, et al. NF1 plexiform neurofibroma growth rate by volumetric MRI: relationship to age and body weight. Neurology. 2007; 68(9):643–647. [PubMed: 17215493]
5. Yang FC, Ingram DA, Chen S, et al. Nf1-dependent tumors require a microenvironment containing Nf1+/-- and c-kit-dependent bone marrow. Cell. 2008; 135(3):437–448. [PubMed: 18984156]
6. Donovan S, Shannon KM, Bollag G. GTPase activating proteins: critical regulators of intracellular signaling. Biochim Biophys Acta. 2002; 1602(1):23–45. [PubMed: 11960693]
7. Sherman L, Atit R, Rosenbaum T, et al. Singel cell Ras-GTP analysis reveals altered Ras activity in a subpopulation of neurofibroma Schwann cells but not fibroblasts. J Biol Chem. 2000; 275(39): 30740–30745. [PubMed: 10900196]
8. Weiss B, Bollag G, Shannon K. Hyperactive Ras as a therapeutic target in neurofibromatosis type 1. Am J Med Genet. 1999; 89(1):14–22. [PubMed: 10469432]
9. Katz D, Lazar A, Lev D. Malignant peripheral nerve sheath tumour (MPNST): the clinical implications of cellular signalling pathways. Expert Rev Mol Med. 2009; 11:e30. [PubMed: 19835664]
10. Carroll SL, Ratner N. How does the Schwann cell lineage form tumors in NF1? Glia. 2008; 56(14): 1590–1605. [PubMed: 18803326]
11. Johannessen CM, Reczek EE, James MF, et al. The NF1 tumor suppressor critically regulates TSC2 and mTOR. Proc Natl Acad Sci U S A. 2005; 102(24):8573–8578. [PubMed: 15937108]
12. Johansson G, Mahller YY, Collins MH, et al. Effective in vivo targeting of the mammalian target of rapamycin pathway in malignant peripheral nerve sheath tumors. Mol Cancer Ther. 2008; 7(5): 1237–1245. [PubMed: 18483311]
13. Wu J, Williams JP, Rizvi TA, et al. Plexiform and dermal neurofibromas and pigmentation are caused by Nf1 loss in desert hedgehog-expressing cells. Cancer Cell. 2008; 13(2):105–116. [PubMed: 18242511]
14. Majumder PK, Febbo PG, Bikoff R, et al. mTOR inhibition reverses Akt-dependent prostate intraepithelial neoplasia through regulation of apoptotic and HIF-1-dependent pathways. Nat Med. 2004; 10(6):594–601. [PubMed: 15156201]
15. Wilhelm SM, Carter C, Tang L, et al. BAY 43-9006 exhibits broad spectrum oral antitumor activity and targets the RAF/MEK/ERK pathway and receptor tyrosine kinases involved in tumor progression and angiogenesis. Cancer Res. 2004; 64(19):7099–7109. [PubMed: 15466206]
16. Guba M, von Breitenbuch P, Steinbauer M, et al. Rapamycin inhibits primary and metastatic tumor growth by antiangiogenesis: involvement of vascular endothelial growth factor. Nat Med. 2002; 8(2):128–135. [PubMed: 11821896]
17. Laplanche R, Meno-Tetang GM, Kawai R. Physiologically based pharmacokinetic (PBPK) modeling of everolimus (RAD001) in rats involving non-linear tissue uptake. J Pharmacokinet Pharmacodyn. 2007; 34(3):373–400. [PubMed: 17431753]
18. Wilhelm S, Chien DS. BAY 43-9006: preclinical data. Curr Pharm Des. 2002; 8(25):2255–2257. [PubMed: 12369853]
19. Huynh H, Lee JW, Chow PK, et al. Sorafenib induces growth suppression in mouse models of gastrointestinal stromal tumor. Mol Cancer Ther. 2009; 8(1):152–159. [PubMed: 19139124]
20. Wu J, Crimmins J, Monk K, et al. Perinatal epidermal growth factor receptor blockade prevents peripheral nerve disruption in a mouse model reminiscent of benign world health organization grade I neurofibroma. Am J Pathol. 2006; 168(5):1686–1696. [PubMed: 16651634]
21. Jain DS, Subbaiah G, Sanyal M, et al. An extensive study on isosorbide-5-mononitrate acid adducts for quantification in human plasma using liquid chromatography/electrospray ionization tandem mass spectrometry and its application to bioequivalence sample analysis. Rapid Commun Mass Spectrom. 2006; 20(19):2921–2931. [PubMed: 16941726]
22. Heitjan DF, Manni A, Santen RJ. Statistical analysis of in vivo tumor growth experiments. Cancer Res. 1993; 53(24):6042–6050. [PubMed: 8261420]

23. Jiang YP, Ballou LM, Lin RZ. Rapamycin-insensitive regulation of 4e-BP1 in regenerating rat liver. J Biol Chem. 2001; 276(14):10943–10951. [PubMed: 11278364]

24. Sparidans RW, Vlaming ML, Lagas JS, et al. Liquid chromatography-tandem mass spectrometric assay for sorafenib and sorafenib-glucuronide in mouse plasma and liver homogenate and identification of the glucuronide metabolite. J Chromatogr B Analyt Technol Biomed Life Sci. 2009; 877(3):269–276.

25. Weiss B, Fisher M, Dombi E, et al. Phase II study of the mTOR inhibitor sirolimus for non-progressive NF1-associated plexifirm neurofibromas: a neurofibromatosis consortium study. Neuro-Oncology. 2010; 12(6):ii1–ii134.

26. Cichowski K, Janne PA. Drug discovery: inhibitors that activate. Nature. 2010; 464(7287):358–359. [PubMed: 20237552]

27. Poulikakos PI, Zhang C, Bollag G, et al. RAF inhibitors transactivate RAF dimers and ERK signalling in cells with wild-type BRAF. Nature. 2010; 464(7287):427–430. [PubMed: 20179705]

28. Hatzivassiliou G, Song K, Yen I, et al. RAF inhibitors prime wild-type RAF to activate the MAPK pathway and enhance growth. Nature. 2010; 464(7287):431–435. [PubMed: 20130576]

29. Heidorn SJ, Milagre C, Whittaker S, et al. Kinase-dead BRAF and oncogenic RAS cooperate to drive tumor progression through CRAF. Cell. 2010; 140(2):209–221. [PubMed: 20141835]

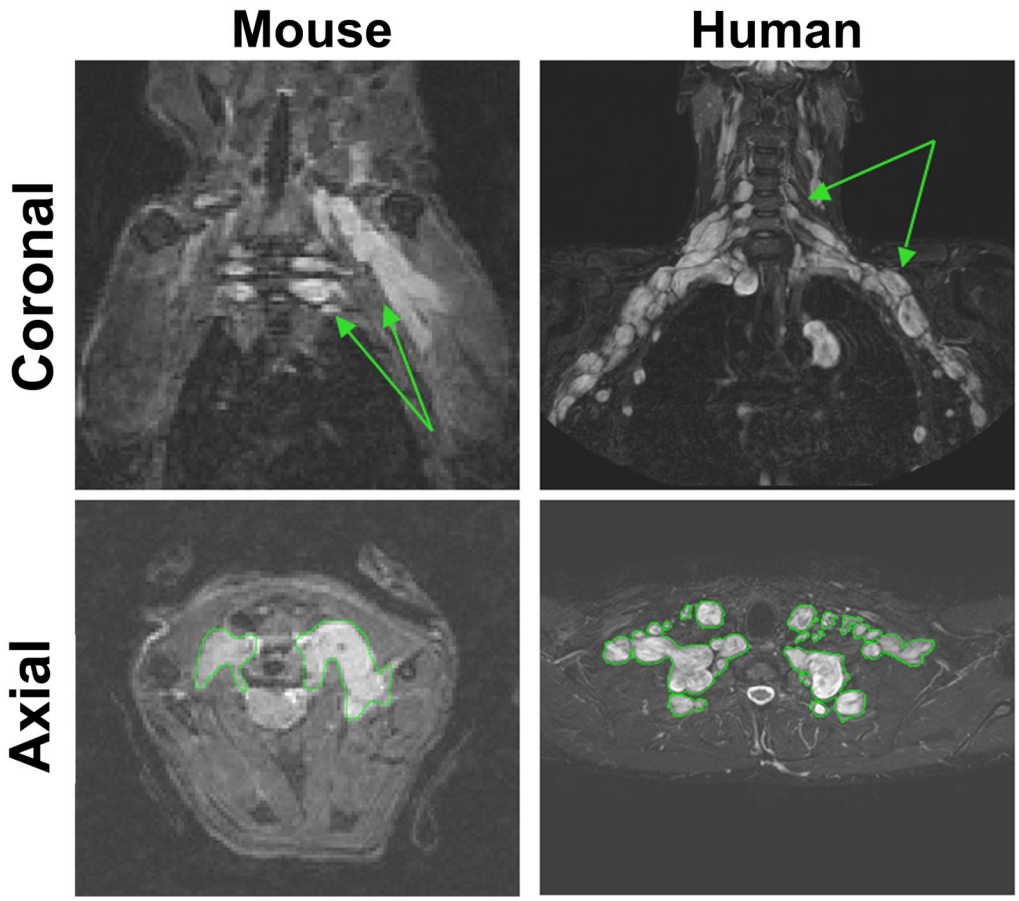

Figure 1. Mouse paraspinal plexiform neurofibromas are similar to human neurofibromas on MRI

Left panels show coronal (top) and axial (bottom) mouse cervical neurofibromas. Arrows denote hyperintense plexiform neurofibroma. Right panels show coronal (top) and axial (bottom) human brachial plexus neurofibroma. For volumetric measurements, tumors were outlined as shown in the bottom panels.

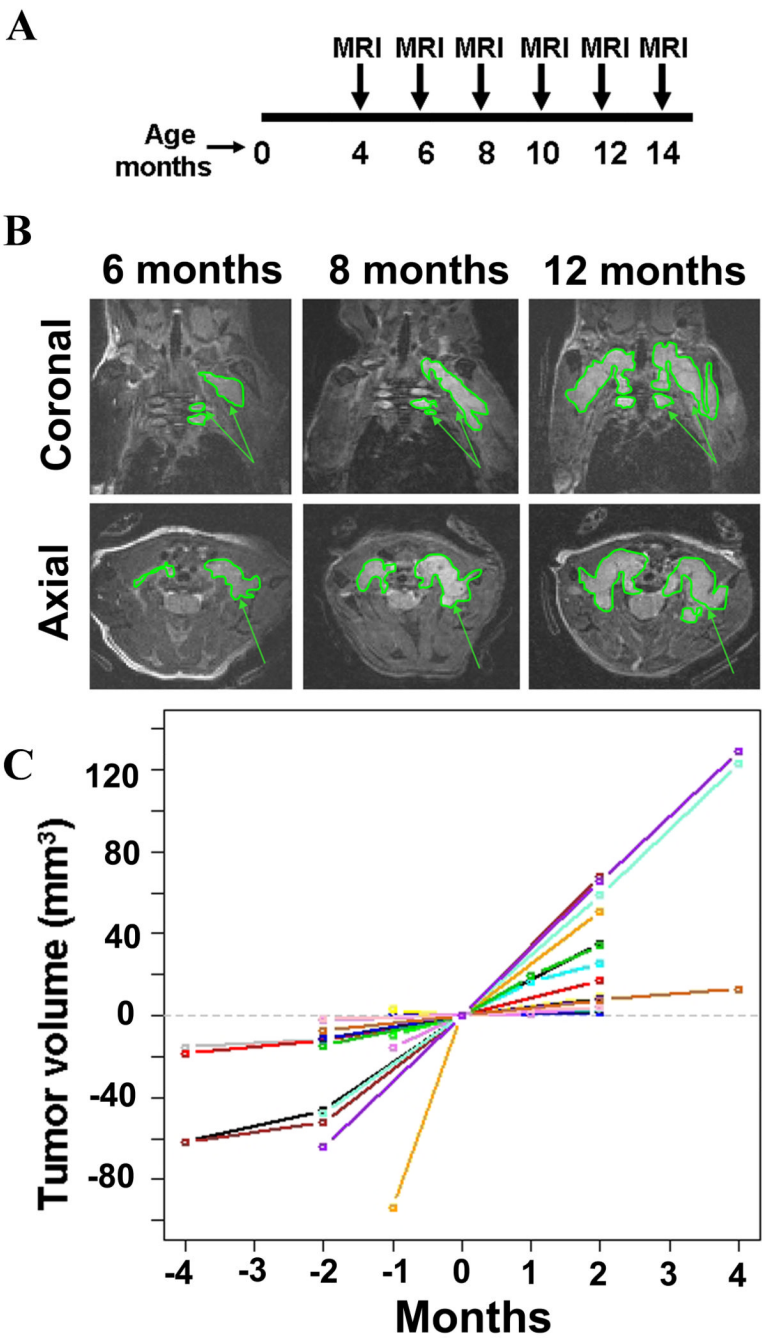

Figure 2. Plexiform neurofibroma development in the *Nf1 flox/flox;DhhCre* mouse monitored by MRI scanning

A: Schema of sequential MRI scans on *Nf1 flox/flox;DhhCre* mice. Mice (n=5) were MRI scanned at 4, 6, 8, 10, 12, 14 months of age. B. Top row shows coronal and bottom row shows axial images of cervical spine taken from the same mouse at 6, 8 and 12 months of age. Tumors are outlined. Arrows denote plexiform tumors. C. Quantification of tumor volume **(in mm^3)** measured by volumetric measurement on *Nf1 flox/flox;DhhCre* mice. The data showed are pooled from this natural history study, the RAD001 trial, Sorafenib trial, and other trials. The x-axis is time in months and y-axis is plexiform neurofibroma tumor volume in mL (mm^3). We defined 0 as the time at which drug treatment started, time before

the treatment as minus, after the treatment as plus (in months). Tumor volumes for each mouse at time 0 were adjusted to 0 on the y axis. Thus the y axis reflects changes from time 0 volume in mm^3.

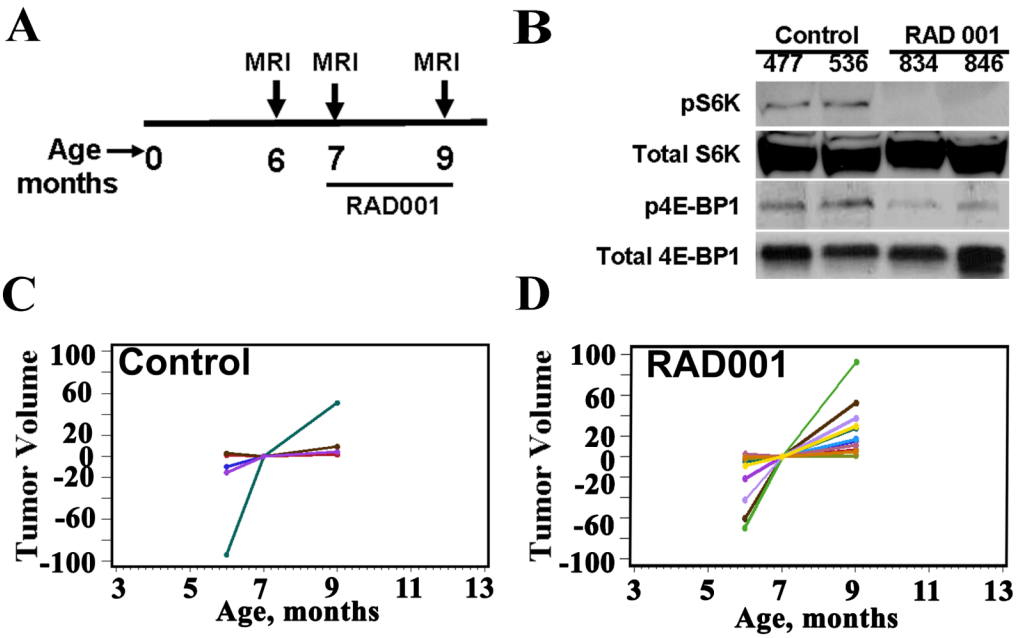

Figure 3.

Volumetric measurements of effects of RAD001 on the *Nf1*$^{flox/flox}$*;DhhCre* mouse. A. Diagram of *Nf1* $^{flox/flox}$*;DhhCre* mouse MRI scanning and RAD001 treatment schedule. B. Western blots showed that RAD001 inhibited phospho-S6 kinase (pS6K) and 4E-BP1 phosphorylation in *Nf1* $^{flox/flox}$*;DhhCre* mouse neurofibromas at the end of the 2 months treatment trial. Total S6K was used as a loading control. C, D. Volumetric measurement on mice treated with vehicle (C, n=4) or RAD001 (D, n=10).

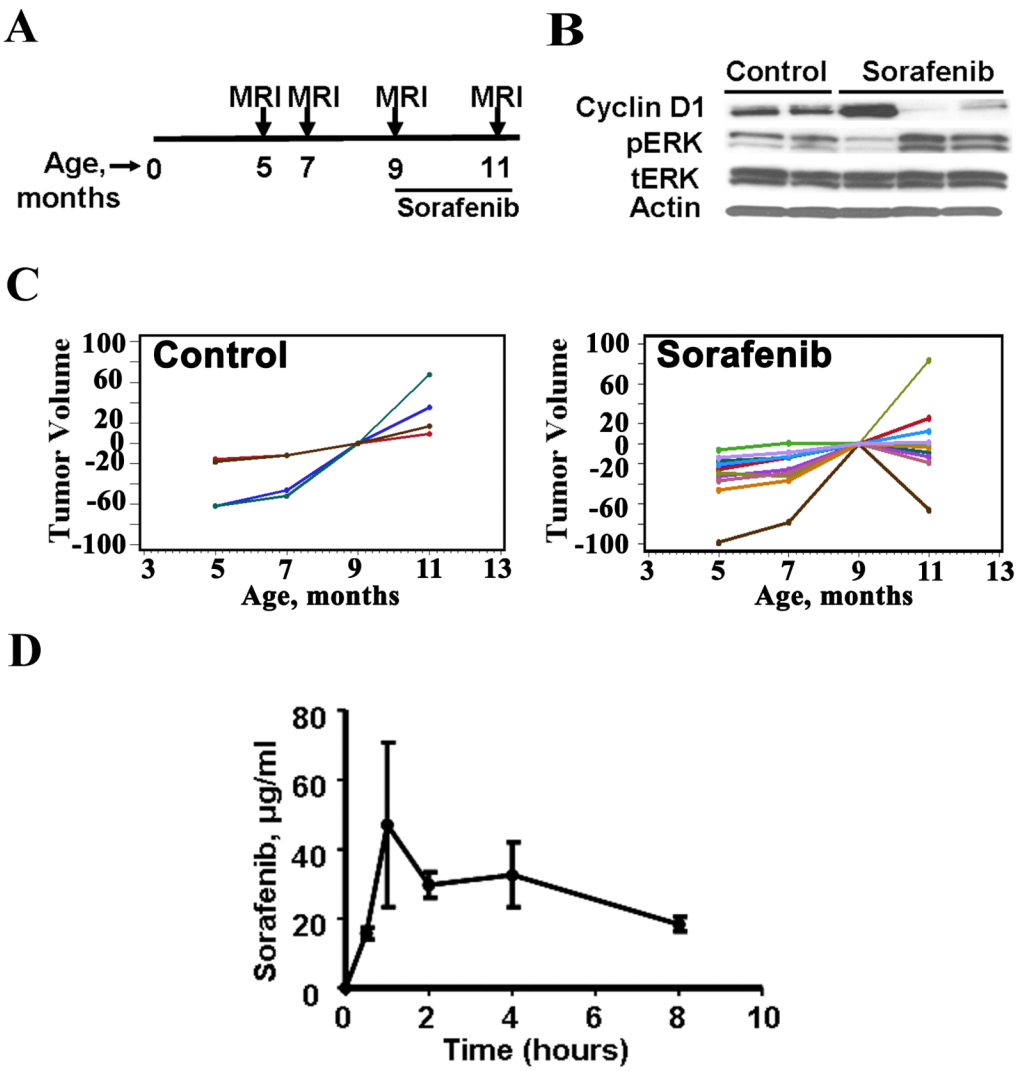

Figure 4. Volumetric measurements show a significant effect of Sorafenib on the *Nf1 flox/flox;DhhCre* mouse tumor growth rate

A. Diagram of *Nf1 flox/flox;DhhCre* mouse MRI scanning and Sorafenib treatment schedule. B. Pharmacodynamic study of Sorafenib in *Nf1 flox/flox;DhhCre* mice. Western blots showed that Sorafenib inhibited cyclin D1 and induced pERK protein expression in *Nf1 flox/flox;DhhCre* mouse neurofibromas at the end of mouse treatment. β-actin and total ERK were used as loading controls. C. Volumetric measurements of mice treated with vehicle (left, n=4) or Sorafenib (right, n=9). D. Pharmacokinetics of Sorafenib in mouse. Sorafenib concentration in mouse plasma samples after oral administration of 45mg/kg Sorafenib by *Nf1 flox/flox;DhhCre* mouse wild type littermates performed at times 0.5, 1, 2, 4, and 8 hours (n=3 per time point, ±SEM).

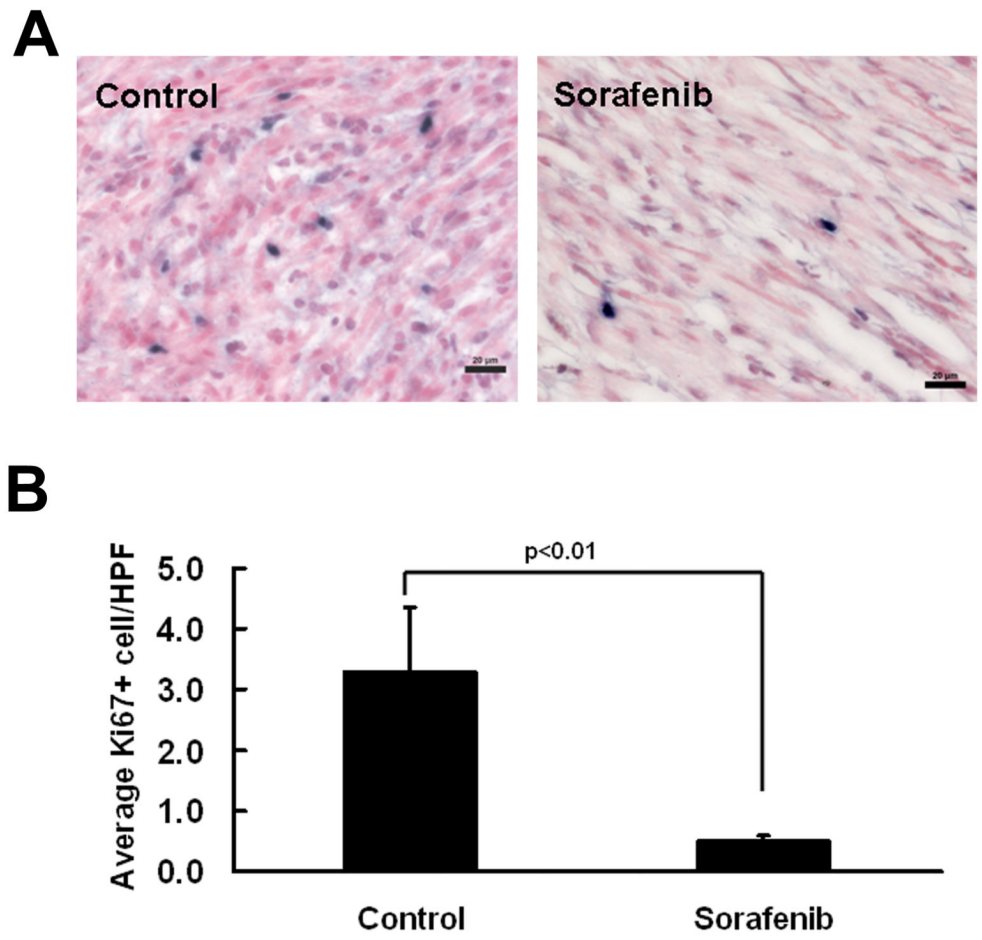

Figure 5. Sorafenib treatment results in decreased tumor cell proliferation

A. Immunostaining with Ki-67 (MIB-1) shows significantly decreased proliferation (Ki-67+ cells; blue) in the GEM-grade neurofibromas from Sorafenib-treated mice (right) compared with vehicle treated mice (left). B. Quantification shows that there is a significant decrease in cell proliferation in Sorafenib treated GEM-grade neurofibromas (n=4, right) compared to vehicle treated mice (n=4, left). Bar, 20 μm.